

Ferromagnetic and antiferromagnetic couplings in Cr(0 0 1) thin films and TM monolayer/Cr(0 0 1) (TM = Ti, V, Cr, Mn, Fe, Co, Ni)

A. Kellou^a, N.E. Fenineche^b, A. Tadjer^a, H. Aourag^{a,b,*}

^a C.M.S.L., Research Center of University, Faculty of Sciences, University of Sidi-Bel-Abbès, Sidi-Bel-Abbès 22000, Algeria

^b LERMPS, Université de Belfort-Montbéliard, Site de Sévenans, Belfort 90010, France

Received 12 April 2002; received in revised form 2 August 2002; accepted 26 September 2002

Abstract

Magnetic and electronic properties of Cr(001) thin films and transition metal monolayer (TM = Ti, V, Cr, Mn, Fe, Co, and Ni) on Cr(001) substrate are reported and discussed within the framework of first principle method based on density functional theory (DFT). In our calculations, we have considered two possible spin orientations leading to ferromagnetic (FM) and antiferromagnetic (AFM) coupling. The surface energy of Cr(001) is given and compared to experimental 4d metals values. Also, total and formation energies, total and local magnetic moments of TM/Cr(001) are determined for both ferromagnetic and antiferromagnetic configurations and compared to other works. Thus, Cr layers in Cr(001) thin films remain antiferromagnetically coupled, as in bulk Cr or Cr₂ molecule. The same behavior is found for Ti, V, and Cr in TM/Cr(001), quite the opposite, Mn, Fe, Co, and Ni prefer to be ferromagnetically coupled to Cr subsurface layer, and only Mn and Fe in the ferromagnetic coupling have induced a spin-switch in all Cr layers. We have also reported the polarized densities of states of each layer in the ground state of TM/Cr(001) systems, showing the same behavior as concluded from energy and magnetic results.

© 2002 Elsevier Science B.V. All rights reserved.

Keywords: Ferromagnetic coupling; Antiferromagnetic coupling; Cr(001) thin films

1. Introduction

During the past decades, the magnetic thin films and layered structures have attracted considerable attention in theoretical and applied physics, storage device technology, and basic research [1,2]. These systems exhibit novel physical phenomena such as giant magneto-resistance [3], enhanced magnetic moments [4], magneto-crystalline anisotropy [5], spin-density waves (SDW) and oscillatory interlayer coupling [6,7].

Several theoretical and experimental studies were devoted to the surface and interface properties of the magnetic 3d transition metal grown on noble metal substrates [8–12]. It is well established that (001) surface of fcc Cu, Ag and Au allow for good epitaxy because many bcc transition metals, such as Cr and Fe, are lattice matched to them by a factor of $\sqrt{2}$, thereby providing a one-on-one match for the atoms at the interface. Also, ferromagnetic substrates, such as Fe(100), have been subject to a great number of studies, where the magnetism of transition metals as overlayer

is interpreted [13–18]. Asada et al. [19] have determined the ground-state spin configurations and the total energies of 3d transition-metal monolayer and bilayer films on Fe(001) within the $c(2 \times 2)$ unit cell. They found that V, Cr, and Mn layers prefer the layered antiferromagnetic (AFM), and Fe, Co, and Ni layers favor the ferromagnetic (FM) coupling to Fe(001). However, it is fair to state that there was not much theoretical progress made on the understanding of ultra thin magnetic films on antiferromagnetic substrates such as Cr. In such systems, the ferromagnetic (FM) ordering can be induced in epitaxial (pseudomorphic) monolayers which otherwise would be nonmagnetic (NM) or antiferromagnetic (AFM), and the magnetic moments are coupled either parallel or antiparallel to the substrate. In addition, this coupling is influenced by film strain, d-band occupancy, and temperature effects. This fact was already reported in several theoretical and experimental studies that were given in order to see the effects of the interfaces and to understand the magnetic properties of thin films [20–23]. For example, Uzdin [24] has reported the strong correlation between distribution of d-electron magnetic moments and the hyperfine fields for Fe/Cr multilayers with different interface roughness, using the Periodic Anderson Model (PAM).

* Corresponding author.

E-mail address: hafid.aourag@utbm.fr (H. Aourag).

However, the magnetic behavior of Cr layers in superlattice, sandwich structures, and artificial close-packed films has been shown to be particularly complex and strongly sensitive to the growth preparations [4,25–28]. In this study, we have studied total and surface energies of Cr(001) films, magnetic, and electronic properties of 3d transition-metal (Ti, V, Cr, Mn, Fe, Co, Ni) monolayer on Cr(001), with two opposite spin orientations leading to ferromagnetic and antiferromagnetic configurations.

Our paper is organized as follows: in Section 2, we give details of the calculations and geometry of the layered structures. In Section 3, we present surface energies, magnetic moments of three- and five-layers of Cr(001), and total energies and magnetic moments for ferromagnetic and antiferromagnetic couplings of TM/Cr(001) systems. Also, spin-resolved densities of states of the ground-state are discussed. Finally, in Section 4 we give a global review of obtained results as some concluding remarks.

2. Details and structures used in the calculations

In this present calculations, we have used as structure five-layers Cr(001) in repeated slab structure. The lateral lattice constant a was taken from the optimized bulk value of bcc Cr ($a = 2.87 \text{ \AA}$). We have incorporated several vacuum layers between the up and down slabs in the supercell. The slabs are symmetric with respect to the central substrate layer to avoid any charge accumulation on the surfaces [29–31]. Fig. 1(a) and (b) represent the side view of three- and five-layers of Cr(001) films, respectively, and Fig. 1(c) represents the half-slab of TM/Cr(001) unit cell (TM = Ti, V, Cr, Mn, Fe, Co, Ni).

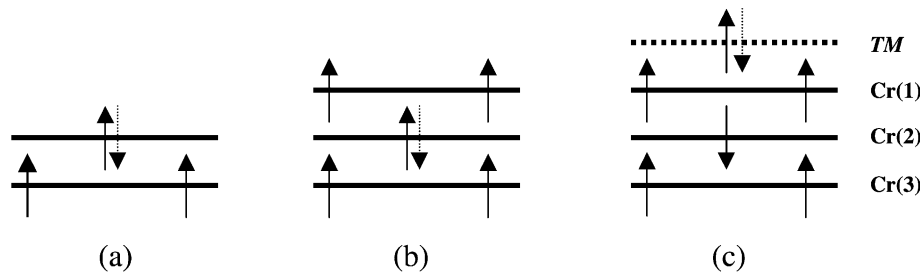


Fig. 1. Down half-slab of the unit cell in: (a) 3-Cr(001), (b) 5-Cr(001), and (c) TM/Cr(001). Up (+) and down (–) arrows refer to ferromagnetic and antiferromagnetic configurations, respectively.

Table 1

Total energies difference (ΔE) relative to energy of antiferromagnetic bcc structure of Cr (-2101.77480 Ry per atom), surface energy per atom (γ_{100}), magnetic moments of first, second, and third layers (M_1 , M_2 , and M_3), and total magnetic moment (M) including interstitial region for the layered Cr(001) systems, as shown in Fig. 1

	ΔE (mRy per atom)	$2\gamma_{100}$ (mRy \AA^{-2})	M_1 (μ_B)	M_2 (μ_B)	M_3 (μ_B)	M (μ_B)
Bulk Cr	0.00	–	+0.77	–0.77	–	0.00
(+ +)	79.063	28.79	–1.92	+2.83	–	+1.67
(+ –)	79.088	28.80	+1.84	–2.82	–	–1.74
(+ – +)	47.240	28.67	+1.17	–1.53	+2.60	+2.85
(+ + +)	47.216	28.66	+1.33	–1.64	+2.63	+1.93

All energy calculations were carried out using a self-consistence scheme with scalar-relativistic version of the Full-Potential Linearized Augmented Plane Waves (FP-LAPW) [32–35], where the core states were treated fully relativistically in the frozen core approximation. Inside the muffin-tin spheres, the wavefunctions, electron charge densities, and potentials are expanded in terms of the spherical harmonics, while for the interstitial region between the spheres plane-wave expansions are used. The muffin-tin radii of the selected TM family were taken as 2.10, 2.15, 2.20, 2.25, 2.3, 2.35, and 2.40 a.u. for Ti, V, Cr, Mn, Fe, Co, and Ni, respectively. The gradient-conjugate correction (GCC) functional of Perdew et al. [36] (PBE) to the local spin density approximation (LSDA) was taken to include the exchange-correlation energy without any atomic position relaxation or surface reconstruction. The spin-orbit coupling (SOC) is not taken into account. Also, spin-polarized calculations were achieved with two different spin-up and -down densities and two sets of Kohn–Sham single-particle equations for the two spin component were solved self-consistently.

3. Results

3.1. Clean Cr(001) thin film

The total energies, surface energies, and local and magnetic moments of Cr(001) films are listed in Table 1. The signs (+) and (–) refer to up and down initial spin orientation, respectively, for 3-Cr(001) and 5-Cr(001) (see Fig. 1). Although bulk Cr is not a ferromagnet, we have found that its ground state is antiferromagnetic, as already reported in

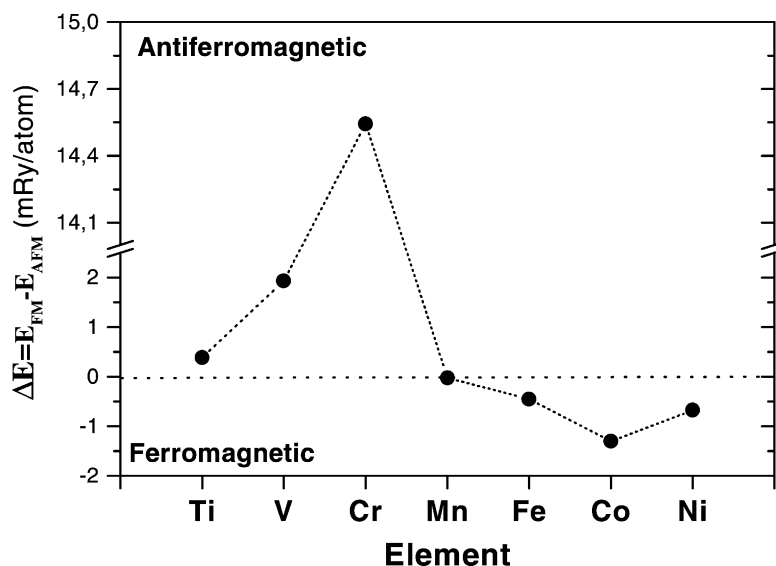


Fig. 2. Variation of the difference of the total energy (between ferromagnetic and antiferromagnetic energies) with the atomic number Z . Positive (negative) values refer to antiferromagnetic (ferromagnetic) coupling.

previous papers [25,26]. The calculated local magnetic moments of bulk Cr are in good agreement with the experimental value of bcc-Cr ($0.61 \mu_B$). As shown in Table 1, the general trend is that local magnetic moment on each atom decreases from the surface layer atom to the central one. The total magnetic moment of (+ - +) configuration is more important than (+ + +) configuration and represent 4.67 of the experimental value. Nevertheless, the formation energy, relatively to the bulk value, reveals that the ferromagnetic coupling is more suitable than the antiferromagnetic one. However, the energy differences are very close to each other, and were calculated without taking into account any relaxation or optimization scheme. The magnetic moment of the surface layer ($M_3 = 2.63 \mu_B$) is equal to the reported value of Bihlmayer et al. ($2.63 \mu_B$) [37]. Thus, as mentioned elsewhere [38], we have found that the (+ - +) configuration is more suitable for five-layers rather than (+ + +) configuration. Also, we have a spin-switch in the second layer in both (+ +) and (+ + +) configurations, which means that the antiferromagnetic order stay in the ground state of the converged energy, as found for bulk Cr and Cr₂ molecule [39]. This predicted antiferromagnetic coupling between Cr layers was confirmed by recent experimental study based on a spin resolved inverse photoemission of Cr ultrathin films (up to few monolayers) grown on Ag(001) at room temperature [40]. Theoretical study also indicates that a $c(2 \times 2)$ antiferromagnetic order is slightly favored over ferromagnetic one in the case of Cr monolayer on Ag(001) [41].

We have also reported the surface energies for all the systems, and we can get an order of the stabilized value around 3.12 J m^{-2} , which is very close to the experimentally values of Nb, Mo, Tc, and Ru, derived by De Boer et al. [42] for the 4d metals.

3.2. TM monolayer on Cr(0 0 1) substrate

In order to get the ground state configuration of all TM/Cr(001) systems, we have reported in Fig. 2 the difference in energy between ferromagnetic and antiferromagnetic states. The positive (negative) values refer to antiferromagnetic (ferromagnetic) coupling between TM overlayer and the subsurface Cr layer (i.e. Cr(3) as shown in Fig. 1). As shown, Ti, V, and Cr are antiferromagnetically coupled to the Cr subsurface layer, but Fe, Co, and Ni are ferromagnetically aligned. Although in the Mn case, the energy difference between antiferromagnetic and ferromagnetic configuration is only about -0.023 m Ry per atom, we can presume that ferromagnetic coupling is the ground state.

In Table 2, the local and interstitial moments are reported for both ferromagnetic (\uparrow) and antiferromagnetic (\downarrow) configurations for the TM/Cr(001) systems. Among the TM materials, only Mn and Fe overlayers have affected the spin

Table 2

Local magnetic moments of first, second, and third layers (M_1 , M_2 , and M_3), and interstitial magnetic moment (M_{int}) of the TM/Cr(001) systems, as represented in Fig. 1

	M_1 (μ_B)		M_2 (μ_B)		M_3 (μ_B)		M_{int} (μ_B)	
	\uparrow	\downarrow	\uparrow	\downarrow	\uparrow	\downarrow	\uparrow	\downarrow
Ti	+0.86	+0.84	-0.66	-0.74	+0.44	+0.79	+0.28	-0.36
V	+0.70	+0.70	-0.57	-0.64	+0.25	+0.71	+0.29	-0.43
Cr	+0.63	+0.93	-0.65	-0.93	+0.36	+1.29	+0.66	-0.55
Mn	-1.12	+1.03	+1.20	-1.09	-1.42	+1.32	+0.49	-0.50
Fe	-1.07	+0.83	+1.05	-0.84	-0.94	+0.80	+0.14	-0.26
Co	+0.44	+0.78	-0.63	-0.71	+0.63	+0.51	-0.04	+0.08
Ni	+0.65	+0.67	-0.79	-0.67	+1.34	0.79	+0.13	+0.06

Up and down arrows refer to ferromagnetic and antiferromagnetic configurations, respectively.

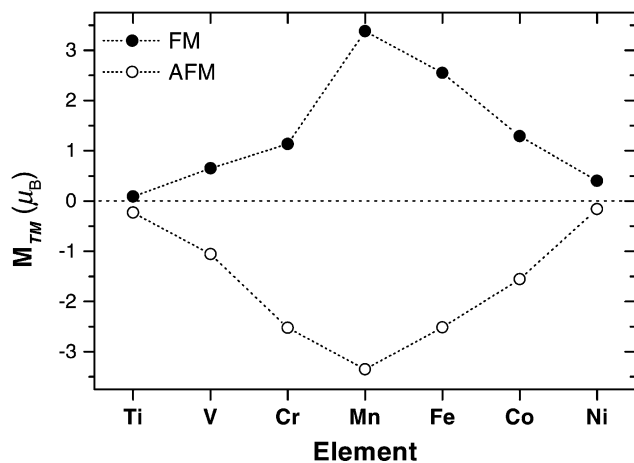


Fig. 3. Variation of the transition metal magnetic moment for Ti to Ni elements. Full and empty circles refer to ferromagnetic (FM) and antiferromagnetic (AFM) coupling, respectively.

direction in the first, second, and third layers. Effectively, in the ferromagnetic state of Mn/Cr(001) and Fe/Cr(001), all the spins are switched when compared to the 5-Cr(001) layers and configuration as shown in Fig. 1(c). However, for the rest of TM materials, all the magnetic moments have kept their initial direction and are aligned as in the 5-Cr(001) layers (including Mn/Cr(001) and Fe/Cr(001) in antiferromagnetic state).

In Fig. 3, the TMs magnetic moment increase from Ti to Mn and decrease from Mn to Ni, in both ferromagnetic and antiferromagnetic configurations. The deposition of the Mn overlayer has induced the highest values of the local magnetic moment, followed by the Fe, Co, and Ni deposition. These induced magnetic moments on the surface layer can be compared to the cited magnetic moments for TMs on both Cu(001) and Au(001) given by the work of Sanyal [43],

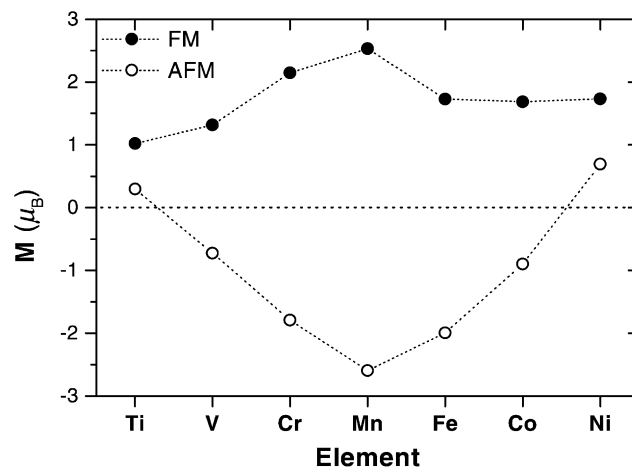


Fig. 4. Variation of the half-slab total magnetic moment (including interstitial region) with the transition-metal element.

which demonstrates several interesting magnetic properties of monoatomic multilayers consisting of 3d transition metals and noble metals Au and Cu stacked in the L₁₀ structure, by quantum mechanics method. In Fig. 3, the obtained peak for Mn on Cr (3.38 μ_B) is less important than Mn on Au (3.89 μ_B) [43] and Mn on Cu (3.75 μ_B) [44]. The measured room temperature value of the Mn magnetic moment for a thin film on Fe range from 1.70 to 4.50 μ_B [45,46], which is larger than the value of 0.60–1.90 μ_B measured for a thin film of Cr on Fe [47]. The calculated value of the Fe magnetic moment on Cr is 2.548 μ_B which is comparable to Fe on Cu (2.53 μ_B) [43], Fe on Mo (2.29 μ_B, 2.37 μ_B, 2.75 μ_B for (001), (111), and (011), respectively) [48], and Fe on W(110) (2.53 μ_B) [49].

In the other hand, the total magnetic moment has the same behavior, as represented in Fig. 4. Nevertheless, Ti and Ni

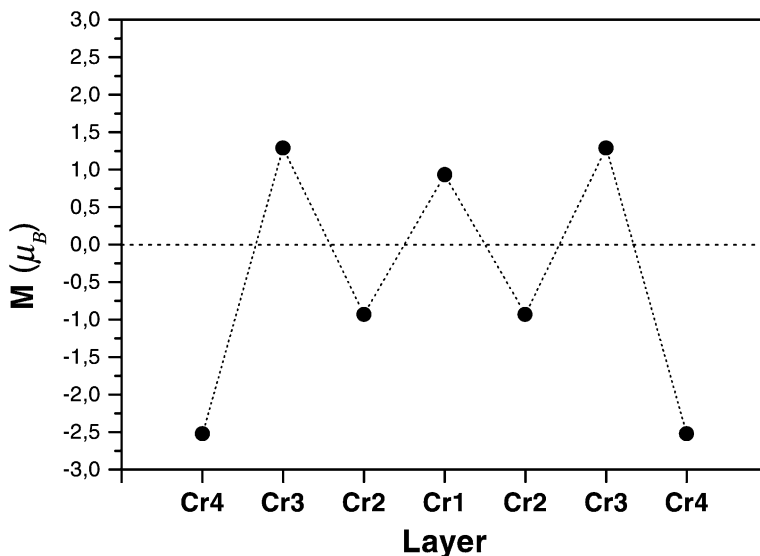


Fig. 5. Local magnetic moments of each Cr atom in 7-Cr(001) layers.

have positive magnetic moments in the AFM state, and Fe, Co, and Ni have similar moments in the FM state. The maximum value in the ferromagnetic configuration (assumed as the ground-state) is also induced by Mn overlayer ($2.53 \mu_B$). Moreover, the total magnetic moment of TM/Cr(001) decreases considerably when compared to the 5-Cr(001) layers; the estimated alteration, relatively to 5-Cr(001) magnetic moment, are as follows: 89.71, 74.61, 37.25, 11.41, 39.46, 40.97, and 39.37%, for Ti, V, Cr, Mn, Fe, Co, and Ni, respectively.

In order to see the alternate antiferromagnetic coupling in Cr films, we have reported the oscillation of the local Cr

magnetic moments of seven-layers as shown in Fig. 5. The periodic nature of these oscillations is strongly related to the itinerant linear spin-density waves (SDW), which was already observed in Cr multilayers [6,7], bulk Cr [50], and its alloys [51]. Consequently, also Cr thin films need SDW to have antiferromagnetic ground state.

Total and partial spin-up and -down densities of states (DOS and PDOS) of TM/Cr(001) are represented in Fig. 6. The spin-up and -down densities are quite different; especially for Mn and Fe overlayers. Even the TM densities of states (PDOS) indicate that the number of states in both up- and down-states is more important in high energies

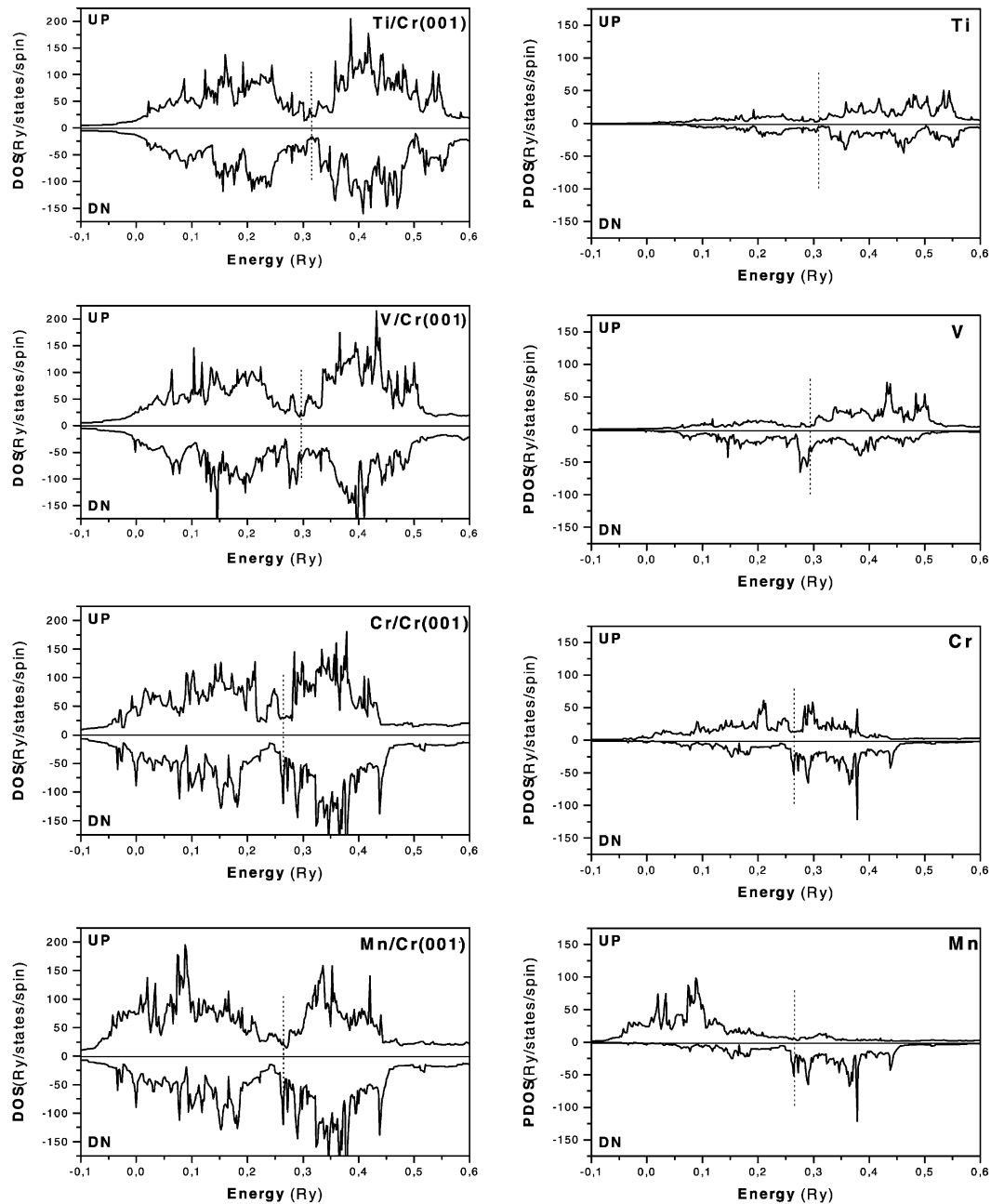


Fig. 6. Spin-resolved total and transition metal densities of state (DOS and PDOS, respectively).

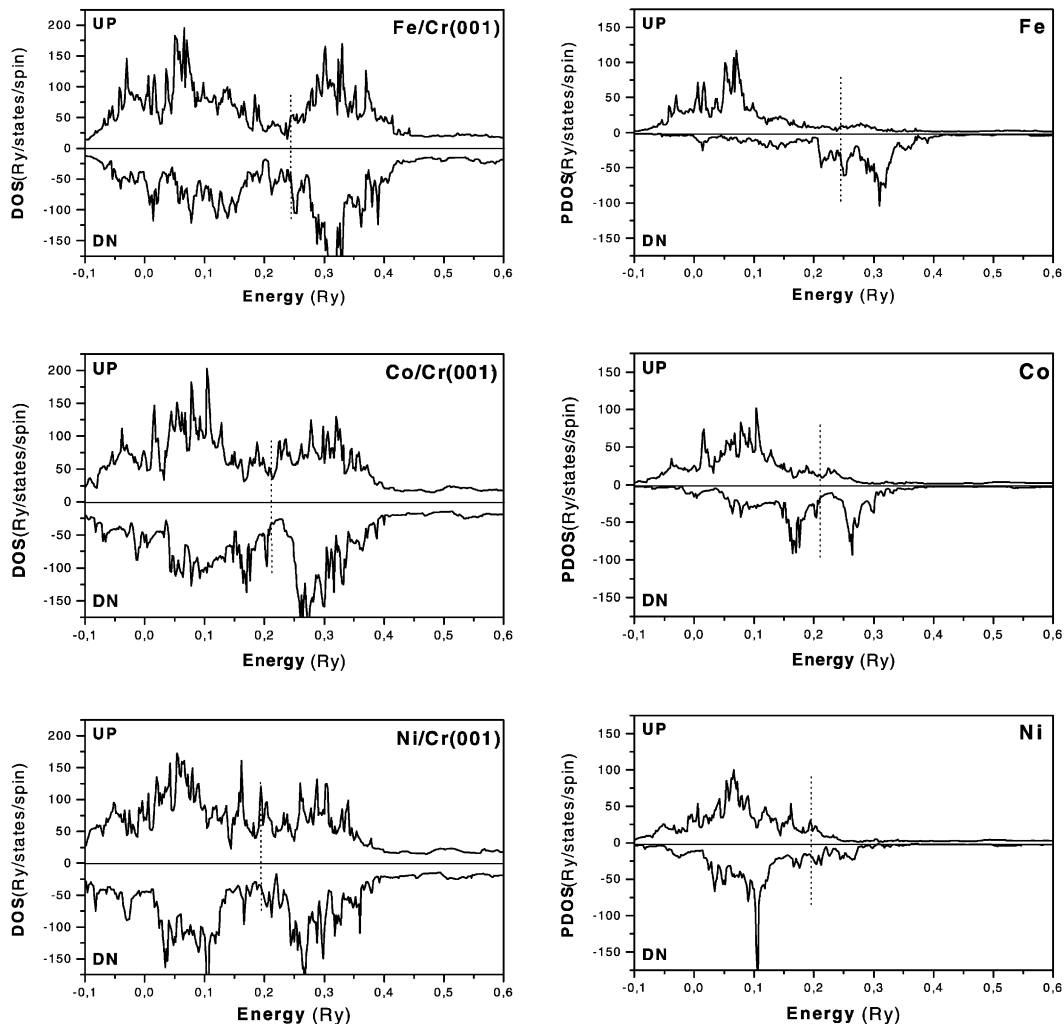


Fig. 6. (Continued).

(unoccupied states) for Ti, V, and Cr, though, the number of the states is more important in low energies (occupied states) for Mn, Fe, Co, and Ni. The contribution of the TM PDOS in the total DOS is quite different from Ti to Ni; PDOS of Ti, V, Cr imply an antiferromagnetic coupling, however, PDOS of Mn, Fe, Co, and Ni imply a ferromagnetic coupling, as also reported earlier.

4. Conclusion

In summary, we have found that surface energy of Cr is close to surface energy of 4d metals, such as Nb, Mo, Tc, and Ru. Moreover, for all Cr thin film with ferromagnetic coupling, we have found that converged total energies are accompanied by a spin-switching between two nearest layers. Thereby, Cr-layered structures, in the existence of itinerant linear spin-density wave (SDW), prefer antiferromagnetic rather than ferromagnetic coupling, as in the bulk of Cr bulk and molecule.

Among the transition metal materials, Mn represents a singular case since it relies between two opposite spin alignments in TM/Cr(001) and, hence, it will not be impossible that ferrimagnetic (FI) coupling can occur or be favorable in Mn/Cr(001) systems. Further investigations within the c (2×2) unit cell are necessary to allow this configuration. In addition, Ti, V, and Cr overlayers are antiferromagnetically coupled to the Cr subsurface layer; Mn, Fe, Co and Ni are ferromagnetically coupled. Also, Mn overlayer induces the highest magnetic moments, and only ferromagnetic Mn and Fe induce the spin-switch in all Cr layers. However, when we compare Fe/Cr(001) to Cr/Fe(001), we can notice that Cr is coupled to Fe subsurface layer in Cr/Fe(001) [19] without spin-switching, which is quite opposite to Fe on Cr(001) substrate.

We can also mention that the deposition of transition metal overlayer on Cr(001) substrate, antiferromagnetic coupling between TM and subsurface Cr layer reduce considerably the total magnetic moment of TM/Cr(001) systems.

References

- [1] R.F.C. Farrow, B. Dieny, M. Donath, A. Fert, B.D. Hermsmeier (Eds.), *Magnetism and Structure in Systems of Reduced Dimensions*, Plenum Press, New York, 1993.
- [2] J.A.C. Bland, B. Heinrich (Eds.), *Ultrathin Magnetic Structures*, Springer, New York, 1994.
- [3] P. Grünberg, R. Shreiber, P. Yang, M.B. Brodsky, H. Sowers, *Phys. Rev. Lett.* 57 (1986) 2442.
- [4] C. Turtur, G. Bayreuther, *Phys. Rev. Lett.* 72 (1994) 1557, and references therein.
- [5] P. Bruno, *Phys. Rev. B* 39 (1988) 865.
- [6] R.S. Fishman, *J. Phys. Condens. Mater.* 13 (2001) R235.
- [7] J.A.C. Bland, B. Heinrich (Eds.), *Ultrathin Magnetic Structures*, Springer, Berlin, 1994.
- [8] M. Eder, J. Hafner, E.G. Moroni, *Phys. Rev. B* 61 (2000) 11492.
- [9] J. Giergiel, J. Shen, J. Wolterdorf, A. Kirilyuk, J. Kirshner, *Phys. Rev. B* 52 (1995) 8528.
- [10] B. Sanyal, *Phys. Stat. Sol. B* 221 (2000) 713.
- [11] B. Heinrich, J.F. Cochran, *Adv. Phys.* 42 (1993) 523, and references therein.
- [12] R.E. Camley, D. Li, *Phys. Rev. Lett.* 84 (2000) 4709.
- [13] S. Handschuh, S. Blügel, *Solid State Commun.* 105 (1998) 633.
- [14] T.G. Walker, H. Hopster, *Phys. Rev. B* 72 (1994) 1557; T.G. Walker, H. Hopster, *Phys. Rev. B* 48 (1993) 3563.
- [15] S.T. Purcell, et al., *Phys. Rev. B* 45 (1992) 13064.
- [16] J. Vogel, G. Panaccione, M. Sacchi, *Phys. Rev. B* 50 (1994) 7157.
- [17] P. Pain, J.P. Eymery, *J. Magn. Magn. Mater.* 133 (1994) 493.
- [18] D. Spisak, J. Hafner, *Phys. Rev. B* 62 (2000) 9575.
- [19] T. Asada, S. Blügel, G. Bihlmayer, S. Handschuh, R. Abt, *J. Appl. Phys.* 85 (2000) 5935.
- [20] V.M. Uzdin, D. Knabben, F.U. Hillebrecht, E. Kisker, *Phys. Rev. B* 59 (1999) 1214.
- [21] J. Ungiris, R.J. Celotta, D.T. Pierce, *Phys. Rev. Lett.* 69 (1993) 1125.
- [22] T. Boske, W. Clemens, D. Scmitz, J. Kojnok, M. Shafer, V. Cross, G.Y. Guo, W. Eberhardt, *Appl. Phys. A* 61 (1995) 119.
- [23] Ph. Kurz, G. Bihlmayer, S. Blügel, *J. Appl. Phys.* 87 (2000) 6101.
- [24] V.M. Uzdin, *Comput. Mater. Sci.* 17 (2000) 477.
- [25] G.Y. Guo, H.H. Wang, *Phys. Rev. B* 62 (2000) 5136.
- [26] H.H. Wang, G.Y. Guo, *J. Magn. Magn. Mater.* 209 (2000) 98.
- [27] B. Heinrich, M. From, J.F. Cochran, M. Kowalewski, D. Atlan, Z. Celinski, K. Myrthe, *J. Magn. Magn. Mater.* 140–144 (1995) 545.
- [28] A. Berger, H. Hopster, *Phys. Rev. Lett.* 73 (1994) 193.
- [29] X. Qian, F. Wagner, M. Peterson, W. Hüber, *J. Magn. Magn. Mater.* 213 (2000) 12.
- [30] B. Kohler, S. Wilke, M. Scheffler, K. Kouba, C. Ambrosch-Draxl, *Comput. Phys. Commun.* 94 (1996) 31.
- [31] B. Kohler, P. Ruggerone, M. Scheffler, *Phys. Rev. B* 56 (1997) 13503.
- [32] P. Blaha, K. Schwarz, J. Luitz, WIEN 97, Vienna University of Technology, Vienna, 1997; P. Blaha, K. Schwarz, P. Sorantin, S.B. Trickey, *Comput. Phys. Commun.* 59 (1990) 399.
- [33] O.K. Anderson, *Solid State Commun.* 13 (1973) 133.
- [34] D.D. Koelling, B.N. Harmon, *J. Phys. C* 10 (1977) 3170.
- [35] D.D. Koelling, G.O. Arbman, *J. Phys. Part F. Met. Phys.* 5 (1975) 2041.
- [36] J.P. Perdew, J.A. Chevary, S.H. Vosko, K.A. Jackson, M.R. Pederson, D.J. Singh, C. Fiolhais, *Phys. Rev. B* 46 (1992) 6671; J.P. Perdew, K. Burke, M. Ernzerhof, *Phys. Rev. Lett.* 77 (1996) 3865.
- [37] G. Bihlmayer, T. Asada, S. Blügel, *Phys. Rev. B* 62 (2000) R11937.
- [38] A. Kellou, H. Aourag, *Phys. Status Solidi B* (2002).
- [39] B. Delley, A.J. Freeman, D.E. Ellis, *Phys. Rev. Lett.* 50 (1983) 488.
- [40] G. Isella, R. Bertacco, M. Zani, L. Duo, F. Ciccaci, *Solid State Commun.* 116 (2000) 283.
- [41] S. Blügel, B. Drittler, R. Zeller, P.H. Dedericks, *Appl. Phys. A* 49 (1989) 547.
- [42] F.R. De Boer, R. Boom, W.C. Mattens, A.R. Miedema, A.K. Niessen, *Cohesion in Metals*, North-Holland, Amsterdam, 1988.
- [43] B. Sanyal, *Phys. Status Solidi B* 221 (2000) 713.
- [44] M. Eder, J. Hafner, E.G. Moroni, *Phys. Rev. B* 61 (2000) 11492.
- [45] S. Andrieu, M. Fanazzi, Ph. Bauer, H. Fisher, P. Lefevre, A. Traverse, K. Hricovini, G. Krill, M. Piecuch, *Phys. Rev. B* 57 (1998) 1985.
- [46] J. Dresselhaus, D. Spanke, F.U. Hillebrecht, E. Kisker, G. Van der Laan, J.B. Goedkoop, N.B. Brookes, *Phys. Rev. B* 56 (1997) 5461.
- [47] P. Fuchs, V.N. Petrov, K. Totland, M. Landolt, *Phys. Rev. B* 54 (1996) 9304.
- [48] B.A. Hamad, J.M. Khalifeh, *Physica B* 321 (2002) 217.
- [49] X. Qian, W. Hübner, *Phys. Rev. B* 60 (1999) 16192.
- [50] E. Fawcett, *Rev. Mod. Phys.* 60 (1988) 209.
- [51] E. Fawcett, H.L. Alberts, V.Yu. Galkin, D.R. Noakes, J.V. Yakhmi, *Rev. Mod. Phys.* 66 (1995) 25.